Acoustic identification of a single transmission at 3115 km from a bottom-mounted source at Kauai

John L. Spiesberger[a)]
Department of Earth and Environmental Science, 240 S. 33rd Street, University of Pennsylvania, Philadelphia, Pennsylvania 19104-6316

(Received 4 October 2002; revised 19 December 2003; accepted 5 January 2004)

Sounds received in the Gulf of Alaska at 3115 km from the ATOC/NPAL source at Kauai (75 Hz, 0.027-s resolution, bottom-mounted) are compared with acoustic and oceanographic models. Unlike data collected at stationary SOSUS arrays, these data come from a towed horizontal array at 372-m depth of military origin. A plausible identification of the acoustic reception is made despite the fact that only one transmission is collected and sound interacts with the bottom near the source. The similarity between the modeled and measured impulse response here may be useful for understanding the signals between this same source and the NPAL array near southern California. The plausible identification of sound from the horizontal array here appears to point toward the feasibility of using other military platforms of opportunity besides SOSUS to study acoustic propagation and possibly map climatic changes in temperature by means of tomography. © *2004 Acoustical Society of America.* [DOI: 10.1121/1.1650014]

PACS numbers: 43.30.Cq, 43.30.Re, 43.30.Pc [RAS]

Pages: 1497–1504

I. INTRODUCTION

Synthetic aperture receivers may yield sufficient resolution to tomographically image climatic temperature variations in the ocean related to El Niño and the Southern Oscillation using signals from a few sources.[1] While sparse sampling may reveal interesting features of climatic change, there may not be enough sound surveillance systems (SOSUS) or other stationary receivers to map these features using tomography without interpolating between sections using a dynamical model of the ocean's circulation.[2] This paper indicates that a towed horizontal array can be used to process and identify acoustic paths over ocean basin scales from a single transmission from the ATOC[3] source at Kauai. Since the received data come from a military origin, it appears that similar arrays could augment stationary receivers to provide a synthetic aperture for mapping climatic variations as the ships move from day to day.

Historically, it was suggested that the mesoscale could be mapped with stationary sources and receivers.[4] A moving source was used to map the mesoscale in a 300 by 300-km^2 area.[5] A moving ship was used to map the mesoscale within a 1000-km-diam circle in the Atlantic.[6] These investigations used instruments with accurate time keeping and navigation.

Mapping the mesoscale seems possible in a mesoscale sized box using inaccurately navigated receivers.[7] Models indicate that synthetic aperture receivers can have location errors of O(1) km and still accurately map climatic variations of temperature such as those due to El Niño and the Southern Oscillation.[1,8] In particular, the simulations suggest that tomographic images of Rossby waves of order O(500) km and other large variations are well resolved using moving receivers with very poor navigation. The effects from a semi-realistic mesoscale are almost negligible in these simulations because of the dominant effects from large scales of temperature on acoustic travel time. These results suggest the possibility of using mobile receivers for studying climate change by means of tomography. A needed demonstration involves processing sounds and identifying acoustic paths that propagate over basin-scales to mobile receivers.

To do tomography between a fixed source on the bottom and mobile receivers, it appears to be useful to investigate two things. First, it is useful to see if acoustic paths can be identified with imperfect information concerning the bottom depth and subbottom properties near the source. It is possible that the difficulty in understanding the acoustic signal between the Kauai source and an array near southern California is due to misunderstood interactions between sound and the bottom near the source *and* the receiver.[3] On the other hand, sounds as received on the towed array discussed in this paper do not interact with the bottom near the receiver, so this geometry is simpler to analyze. A plausible identification is made by assuming that ray paths reflect specularly from the bottom near the source.

Second, it appears necessary to find out if path identification can be made from a single transmission from the source, instead of the traditional method of using numerous transmissions interspersed over a day or longer. With many transmissions, it is possible to average many records to establish stable arrivals that may otherwise fade for a minute or so due to scattering. The fading of acoustic paths is analogous to the twinkling of stars at night due to atmospheric turbulence. The results of this paper support the view that a single transmission can be enough to understand acoustic pulses at the receiver. This appears to be the first time that a model is used to identify signals from a single transmission at basin-scales.

a)Electronic mail: johnsr@sas.upenn.edu

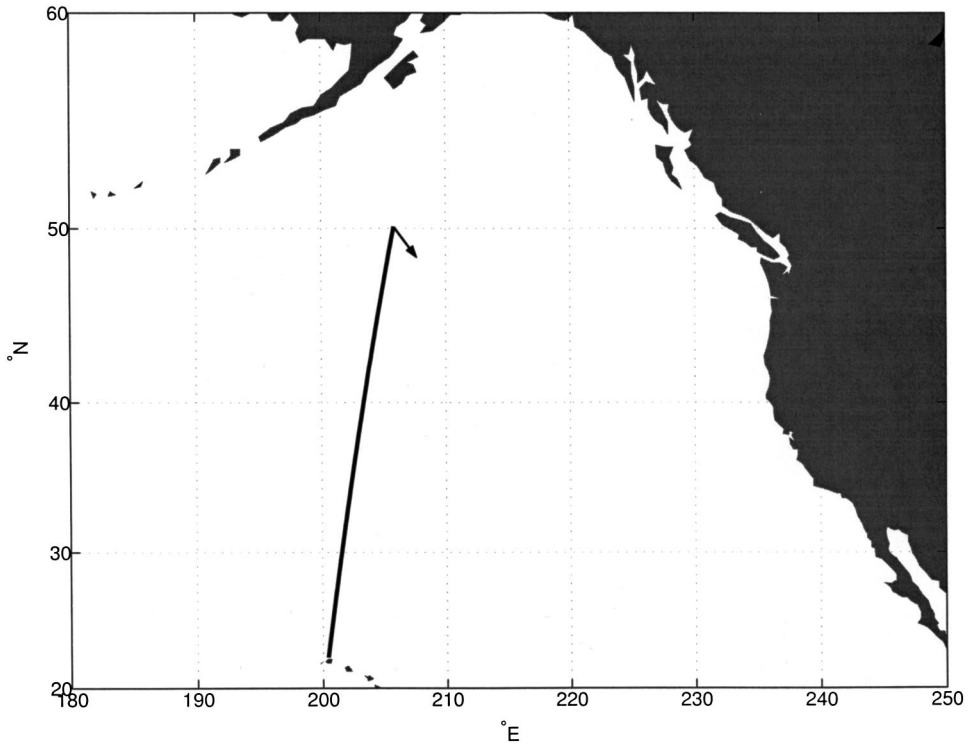

FIG. 1. Plan view of the experiment. Data come from a source at Kauai and are collected on a towed array of U.S. military origin in the Gulf of Alaska. The heading of the vessel is to the southeast and makes an angle of about 53° with the geodesic (arrow).

II. EXPERIMENT

The source[9] is mounted on the bottom at 816-m depth and 22.349°N, 200.43033°E near Kauai. Power and accurate timing are provided through a cable running to the shore. A broadband signal is transmitted at a center frequency of 75 Hz. The phase of the carrier is modulated every two cycles using a linear maximal shift register sequence having 1023 digits. The first zeros in the emitted spectrum are at 75/2 $=37.5$ Hz on either side of 75 Hz. The signal periodicity and level are $(1023)2/75=27.280$ s and 195 dB *re* 1 μPa @ 1 m, respectively. Of the 20 min or 44 transmitted periods beginning at 18:00 on 7 November 1997, 14 min, or 32 periods, are analyzed here.

The receiver is a horizontal array of U.S. military origin towed at 372-m depth. The forward modeling in this paper sets its location at 50.0967°N, 205.8467°E, which is written with much greater precision than its accuracy of a few kilometers. The precision is given so others might model this section using the same coordinates used here.

The geodesic length between the source and receiver is 3115.45 km (Fig. 1). During the arrival of the signal, the array speed is 2.5 m/s and its heading is 137°T. Since the bearing angle to the source is about 190°T, the incoming signal makes an angle of about 53° with respect to the heading of the ship. During the 14 min of data reception, the ship travels 2.2 km and is 1.3 km closer to the source at the end of the 14 min. The data are time stamped with an accuracy of 5 to 10 s. In this paper, it is not possible to compare predictions of acoustic travel time with the data because of the uncertainties of position and timing. However, the sample rate of the data is stable and accurate.

III. DATA

Using standard techniques the data are first beamformed toward the source. Next, each 27.280-s M-sequence period is adjusted for various possible Doppler corrections and correlated with a replica of the transmitted sequence. Replica correlation with a linear maximal shift register sequence compresses 27.280 s of energy from each acoustic path into a pulse of duration $2/75=0.026\,67$ s with a theoretical gain of $10\log_{10}(1023)=30$ dB. The Doppler correction yielding the largest signal-to-noise ratio is chosen for each period. This procedure yields sufficient signal-to-noise ratio to examine the impulse response.

A few words can be said about the coherent integration time of this signal, though it has no bearing on other results in this paper. If one chooses the average Doppler correction among the 32 processed periods, the signal can be coherently integrated for 80 s. It is not known if one could integrate for a longer period than this if one utilized a different Doppler correction for each period. This type of processing would explore the degree to which the ship's change in velocity affects coherent integration time versus effects due to fluctuations in the ocean.

A ''bit plot'' is shown for the output of each of 32 processed periods of the received signal (top, Fig. 2). Some features persist for 14 min and other do not.

Incoherent averages are formed using

$$a(m)=\left[\frac{1}{32}\sum_{r=1}^{32}\frac{\|d(m,r)\|^2}{\sigma^2(r)}\right]^{1/2},\quad m=1,2,\ldots,M, \tag{1}$$

where the mth complex demodulate of the rth record is $d(m,r)$. The variance of the noise for record r is $\sigma^2(r)$. It is included to give proper weight to records based on their signal-to-noise ratio. $\sigma^2(r)$ is estimated from each record where signal is not present. The energy arrives around 2097 s and ends around 2105 s, a duration of 8 s.

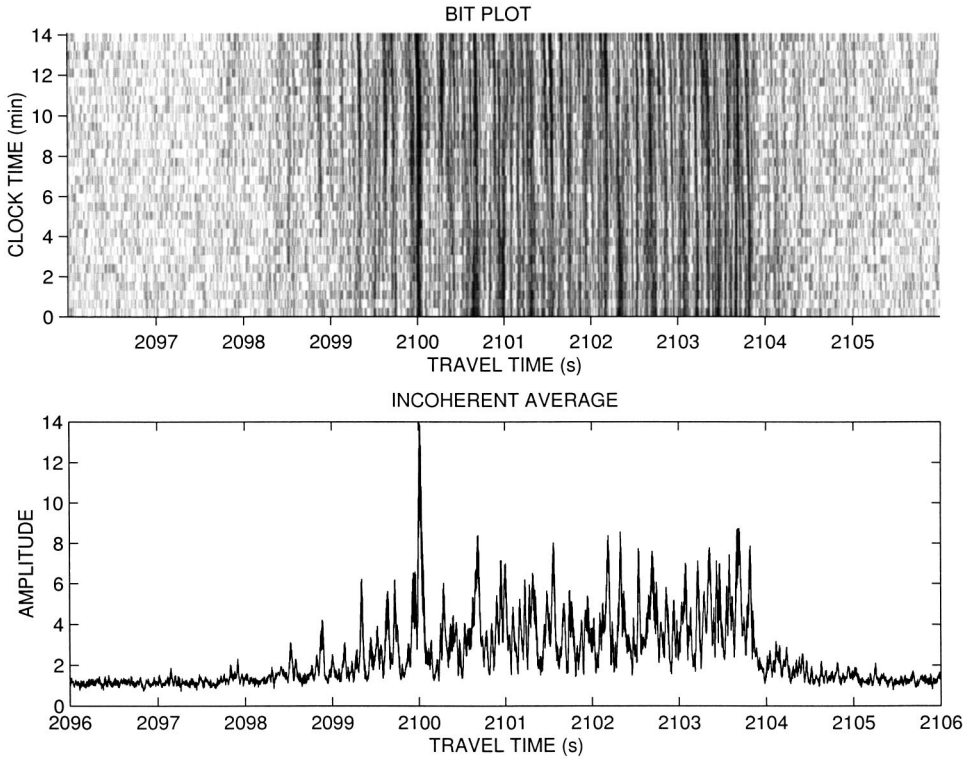

FIG. 2. The impulse response from the Kauai source for the section in Fig. 1 on 7 November 1997. The bit plot shows signal-to-noise ratio from −3 dB and less as white to 20 dB and more as black. Each of the 32 separate periods of received signal, covering a total of 14 min, is separately processed to correct for the motion of the towed array (Doppler) and to remove the shift register sequence code using replica correlation. The bottom panel is the incoherent average [Eq. (1)] of these 32 processed periods. The axis for travel time is inaccurate.

IV. MODELS FOR ACOUSTIC PROPAGATION

Different realizations of the internal wave field are modeled to ascertain their effects on acoustic variability. With previous data, this step has not been needed because many data sets could be averaged to determine the features of the data that were stable and could be expected to be identified from a model. With a single transmission, it is important to model the effects from a time-evolving internal wave field to estimate the portions of the model that ought to be stable and identifiable.

A. Environment

The speed of sound is computed using Del Grosso's algorithm[10] and Levitus' climatological averages[11] of temperature and salinity for Fall. The depth of minimum speed varies from 740 m at the source to 105 m at the receiver. Since the acoustic models use Cartesian coordinates, the sound speed profiles are translated to Cartesian coordinates using the Earth-flattening transformation.

Internal waves are modeled with the Garrett–Munk[12] spectrum. Currents are ignored, being two orders of magnitude less than sound speed perturbations arising from adiabatic vertical displacements of water in the upper ocean. The perturbations are added to the climatology of sound speed described above. Internal wave modes are precomputed and retrieved as needed at range intervals of 80 km to account for changes in water depth, buoyancy frequency, and sound speed. Vertical displacements of these modes are set to zero at the surface and bottom. For each 80-km interval, a three-dimensional field of internal waves is computed in a box of 80 km by 80 km by D m where D is the average depth of the ocean in that interval. A vertical slice through the box gives the vertical displacements along the geodesic. The energy of the internal wave field is taken to be that specified by Garrett and Munk[12] because that energy level has matched observations with this construction of internal waves before.[13] The literature is not unanimous in its adoption of the best energy level to use for acoustic modeling.[14–16] Further information on the construction of internal waves is found elsewhere.[13]

The depth of the bottom near 100 km of the source is taken from a SEABEAM[17] survey (Bruce Howe, personal communication). Beyond this range, depths are taken from a digital database[18] (Fig. 3).

For lack of a definitively better set of parameters for the subbottom near the source, parameters like those used for the Kaneohe source at Oahu[13] are used. The thickness of the sediment is 200 m. The sound speed at the top of the sediment divided by that at the bottom of the water column is 1.02. The density of the sediment is 1.7 gm cm^{-3}. The attenuation in the sediment is

$$\alpha(f) = \alpha_0 f^p (\text{dB m}^{-1}), \tag{2}$$

where f is the frequency in kHz, $p=1$, and $\alpha_0 = 0.02$ dB m^{-1} kHz^{-1}. The speed in the sediment is taken to increase with depth as 1 s^{-1}. The speed in the basement divided by that at the bottom of the sediment layer is 2. The density of the basement layer is 2.5 gm cm^{-3}. The attenuation in the basement is given by Eq. (2) except $\alpha_0 = 0.5$ dB m^{-1} kHz^{-1} and $p=0.1$. Geoacoustic parameters are needed within 500 km of the source because that is where the modeled sound field interacts with the bottom. Most of the interaction occurs in the first 50 km. Afterward, interactions occur with a few deep seamounts.

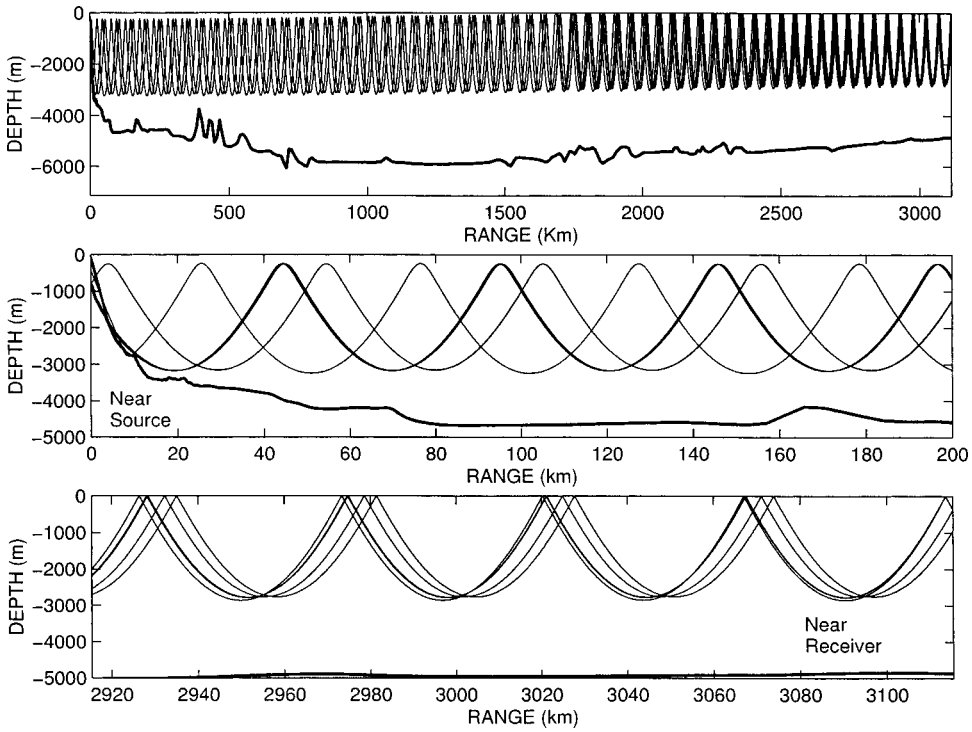

FIG. 3. The depth of the bottom is indicated along the section (Fig. 1) with details near the source and receiver. Rays in the top 16 dB making up arrival B1 in Fig. 7 are indicated.

B. Parabolic approximation

The sound speed insensitive parabolic approximation[19] is used to compute a two-dimensional field of sound along the geodesic from 0- to 8000-m depth. Tests[19] suggest that travel times of pulses are computed with an accuracy of a few milliseconds. The field is modeled at each of 2048 acoustic frequencies. The impulse response is synthesized with an inverse Fourier transform resulting in a time series with a period of 27.3 s. In the first 48 km where sound interacts with the steep slope of Kauai, the computational grid has an interval of 0.0333 km in range and 3.9 m in depth. At greater ranges, the grid interval is 0.1333 km in range and 7.8 m in depth. These values are sufficient to obtain convergence within a few decibels at the receiver.

C. Rays

Fans of rays are traced using a program, zray, that is a modification of ray.[20] Eigenrays are found using another program. These programs have been used to identify acoustic paths before.[21] Rays reflect specularly from the bottom. Both geometric and nongeometric arrivals are found. Geometric types are those that pass through the source and receiver. Nongeometric types are those that provide energy at the receiver on the shadow sides of caustics. For lack of a more reliable value, rays that reflect from the bottom suffer an attenuation of 3 dB per bounce. The sound speed field used for the ray trace is identical to that used for the sound speed insensitive parabolic model at its computational grid.

V. IDENTIFYING ACOUSTIC PATHS

A. Stable arrivals from models

Stable arrivals are those that can be tracked from day to day. This cannot be investigated from one data record. Instead, models are used to predict stability.

Eight impulse responses are computed from the sound speed insensitive parabolic approximation.[19] The sound speed field for each comes from Levitus' climatology and a field of internal waves. Internal waves are generated at intervals of a day using the linear dispersion relation. Two incoherent averages are computed from these eight impulse responses (Fig. 4). Seven stable arrivals are labeled (A–G). Arrivals after 2105 s do not appear to be stable. Arrival C does not look very stable but this is probably because there are not enough model realizations to show its stability. Stable arrivals before A are unlabeled because they have very low signal-to-noise ratios in the data. Arrivals A–D appear to consist of two resolved arrivals, which can be observed in modeled time fronts (Fig. 5). Evidently, at the receiver depth of 372 m, these can be resolved in the presence of the modeled field of internal waves. Temporal separations of later doublets cannot be resolved. Without internal waves, more stable arrivals are predicted than when internal waves are added (Fig. 5). Figure 4 appears to predict stability better than the time fronts, especially between 2104 and 2105 s where it is difficult to judge stability from time fronts.

B. Ray approximation for tomographic inversion

The impulse response from rays looks similar to that from the parabolic approximation (Fig. 6). To use rays for tomographic inversions, it is necessary to show that, for each stable arrival, the corresponding ray paths are themselves sampling a similar region of the ocean and that those ray paths have travel times that are sufficiently accurate.

The first issue can be dealt with by finding the eigenrays for different representations of ocean fields, and examining the paths for each realization for each stable arrival. Our computer resources are insufficient to compute eigenrays through the internal wave field. Investigators have found that at long distances, stable arrivals are composed of many rays.

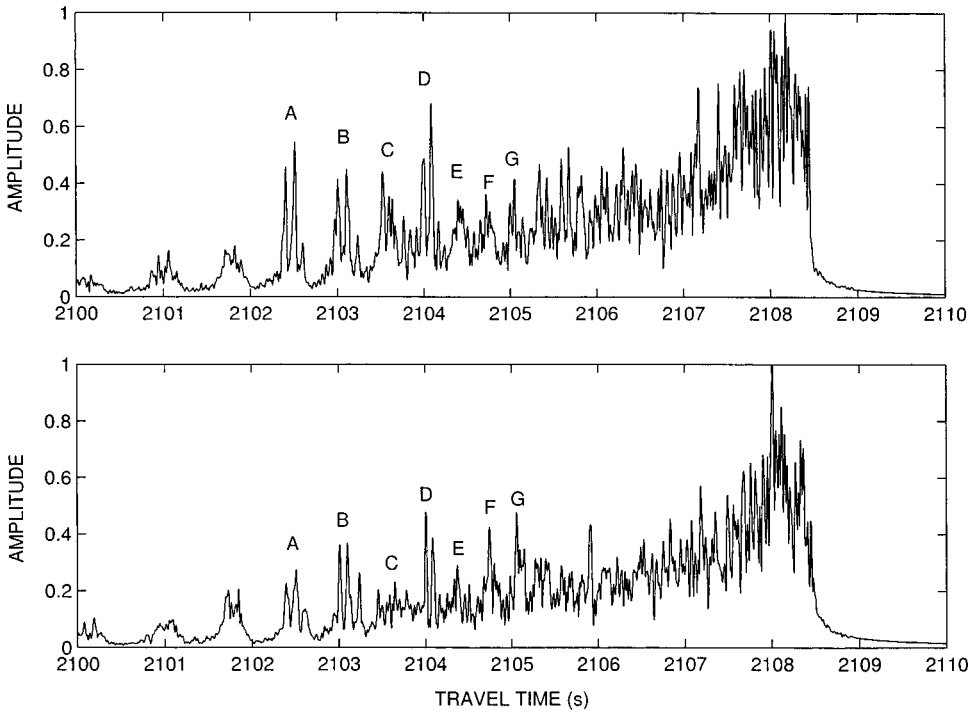

FIG. 4. Investigation of predicted path stability. Top: Incoherent average of four modeled impulse responses at one-day intervals where the modeled time variation is given by the linear dispersion relation and the Garrett–Munk[12] spectrum of internal waves. Bottom: Same except these are from four other impulse responses at one-day intervals. The acoustic receptions are modeled with the sound speed insensitive parabolic approximation.[19] The letters indicate arrivals which appear to be stable from one panel to the next.

Some of the arrivals are suitable for tomographic inversion because their constituent ray paths have similar upper turning depths even though their turning ranges are quite different.[16,21,22] In this experiment, some stable arrivals are composed of several rays (A1, A2, B, C2, D1, E2, F1, F2, G1, G2) even though the mesoscale and internal wave scales are not incorporated into the sound speed field (Fig. 3). The notation ''A1'' or ''A2'' denotes the first or second arrival of a doublet, respectively. Upper turning depths for arrivals A–G are 237 to 358 m, respectively, near the source and 61 to 1 m, respectively, near the receiver. Most stable arrivals appear to be suitable for tomographic inversions.

The second issue is whether the travel times from rays are close enough to a full wave solution of the wave equation to warrant their use without significant modification. In this paper, the full wave solution is given by the parabolic approximation. Travel times of rays and stable arrivals from the parabolic model can differ because of diffraction[23] and due to the fact that the parabolic model includes propagation into the subbottom. Rays are only allowed to reflect specularly from the bottom. Despite these differences, the differences in modeled travel times are less than 0.03 s, and are typically

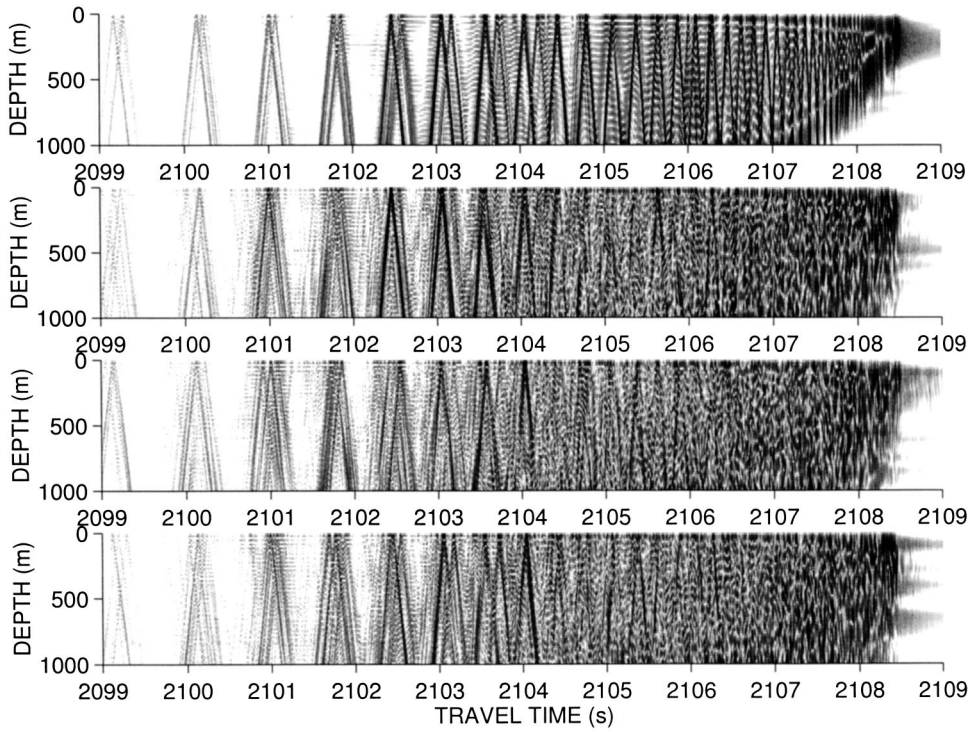

FIG. 5. Modeled time fronts in the top 1000 m at the receiver without internal waves (top) and with internal waves at daily intervals (bottom 3 rows). The receiver is at 372-m depth. The models are generated with the sound speed insensitive parabolic approximation[19] and a Garrett–Munk[12] spectrum of internal waves.

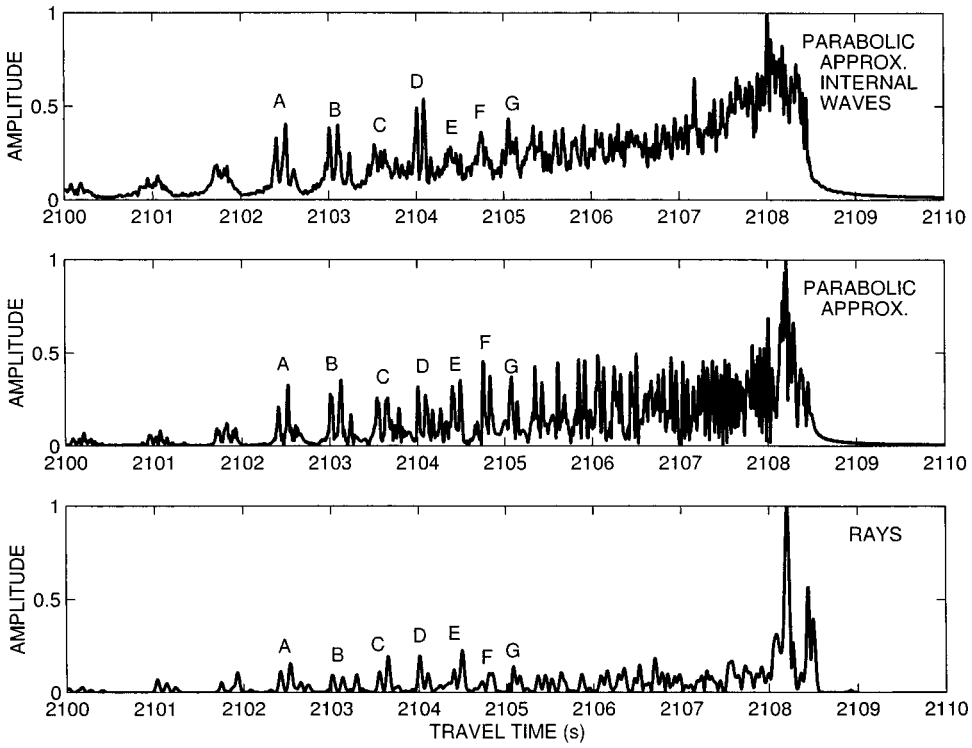

FIG. 6. Three models for the propagation of sound. Top: Same as top panel, Fig. 4 except this uses all eight internal wave fields to construct the incoherent average. Middle: Sound speed insensitive parabolic approximation[19] where the sound speed field is from Levitus' climatology[11] for Fall. Bottom: Eigenrays where the sound speed field is identical to that in the middle panel. The seven arrivals that appear to be stable in the models are labeled A–G.

0.005 s (Table I). These errors are small compared to the climatic signal of about 1 s expected from Rossby waves linked to El Niño and the Southern Oscillation.[2]

C. Identifying arrivals in the data

The most accurate model for identifying paths is the incoherent average of the output from the parabolic equation for eight internal wave fields (Fig. 7). Using a visual alignment, the association with the data is plausible. The seven stable arrivals, A–G, from the model appear in the data. The cutoff times from the data and model are similar, but the data have an extra second of energy at lower levels at the end. This second of energy may come from a positive bias in the travel time of sound that is trapped near the depth of minimum speed in the waveguide. Mesoscale eddies appear to have caused biases of this order in a different transmission at basin-scales.[13]

The lack of an accurate time base probably does not significantly affect the confidence with which the data can be identified with these models because other oceanographic variability associated with ENSO can modify travel times by O(1) s (Ref. 2). With a 1-s error from any model, there is a possibility that the alignment in Fig. 7 is incorrect. However, it appears to be problematic to shift model times earlier or later here because both the data and model exhibit a dramatic drop in level at about 2108.5 s with the alignment in Fig. 7. It is plausible that the "extra energy" that arrives late in Fig. 7 is due to a bias caused by the mesoscale. Thus, the alignment in Fig. 7 is the best one, with other alignments appearing significantly worse. It seems that all acoustic models have difficulty identifying acoustic arrivals from any basin-scale section in the North Pacific without any doubt whatsoever in the face of the inherent O(1) s uncertainty in travel time due to unknown variability at climatic scales.

TABLE I. The difference in travel time between peaks from the parabolic approximation (pe) and ray models from the bottom two panels of Fig. 6. Models are computed for the same sound speed field. Peaks are labeled A-G and the "1" and "2" denote the first and second arrivals of the doublets.

Peak	$T_{pe}-T_{ray}$ (s)
A1	−0.006
A2	−0.009
B1	−0.005
B2	0.
C1	−0.010
C2	−0.014
D1	−0.005
D2	−0.011
E1	−0.003
E2	−0.006
F1	+0.029
F2	−0.008
G1	−0.004
G2	−0.009

VI. CONCLUSIONS

Acoustic signals at 3115 km from a source near Kauai can be coherently processed to yield large signal-to-noise ratios on a towed array in the Gulf of Alaska (Fig. 1). The acoustic paths that are predicted to be stable by means of acoustic and oceanographic models can be identified in the data. There are discrepancies between the models and data, particularly during the last second when weak arrivals are observed that are not present in the model. The models use climatological and internal wave variations, but do not include a mesoscale. A previous study[13] indicates that the mesoscale is responsible for a 0.6-s addition of energy at the end of the reception due to a positive bias in the travel times

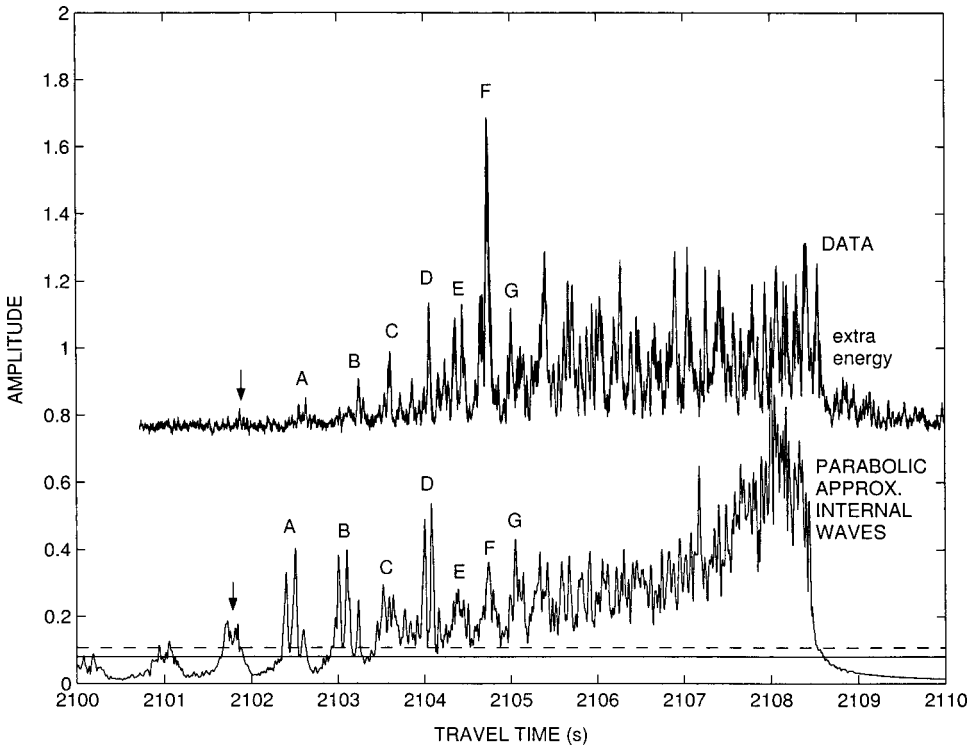

FIG. 7. Incoherent average of the data (Fig. 2) compared with the incoherent average from the parabolic approximation model (top, Fig. 6). Amplitudes of the data are offset so they do not overlap the model. Modeled time variability is generated using eight realizations of the Garrett–Munk[12] spectrum of internal waves at daily intervals. Stable arrivals from the model in Fig. 4 are shown with their associated counterparts from the data. The arrow identifies a weak arrival in the data that corresponds to a modeled arrival. The peak signal-to-noise ratio in the data is 21 dB. The solid line through the model shows this same ratio. The dashed line shows the upper limit for noise variations given the statistical fluctuations of noise in the data. The weak ''extra energy'' in the data is not observed in the model. About 4 s are added to the data to align with the model.

of sounds trapped near the axis of the acoustic waveguide. Unlike internal waves which have a universal spectrum,[12] the mesoscale is not so simply predicted. It is possible that some ocean circulation models have a realistic mesoscale that can be used to predict this bias.

Mobile receivers allow studies of acoustic propagation to be conducted at relatively little cost for many different geographic regions. Although SOSUS stations and the single section studied here yield data that appear to be interpretable with acoustic and oceanographic models, the outcome may be more complicated in different areas of the ocean. Being able to process and identify acoustic paths from the towed array here seems to keep open the possibility of using mobile systems for studying climatic temperature changes in the ocean using tomography and synthetic apertures. Ray models for some identified features from the data here indicate that tomographic inversions are feasible (Fig. 3).

At first thought, inaccurate timing at a receiver may seem to preclude tomography in the ocean. The literature contains a paper showing that models of climatic variability can be accurately mapped from a few sources and 20 mobile receivers even when the time base in the sources is off by hours.[24] The same principles used in that paper could be applied to ask if climatic variability could be mapped if the time bases on mobile receivers were off by hours, but their time bases were stable over months at a time. It is too early to conclude that inaccurate time bases at mobile receivers either could or could not produce accurate maps of climatic variability. On the other hand, accurate timing could be provided for towed arrays if desired.

A significant effort is still required to interpret signals transmitted over basin-scales despite the contemplation of this effort 83 years ago.[25] The process cannot be done in real-time at this point in history. Once a seemingly correct choice of acoustic and oceanographic models is used to identify acoustic paths at a receiver, the computer times required to do the modeling are counted in weeks rather than in the 30 min or so required for the signal to propagate from the source to the receiver. Finding a suitable set of acoustic and oceanographic models usually takes much longer than a few weeks. Perhaps during the next decades, enough experience with other data sets and models will make it possible to accurately predict acoustic signals in many regions of the ocean. The speeds of computation necessary to make predictions will probably not be a limiting factor when predictions can be made reliably and routinely.

The modeled signal penetrates the bottom near the Kauai source. Even though the geoacoustic parameters for this region are currently not well known from the literature, a plausible identification is made at basin-scales, even when the bottom properties are ignored and only specular reflection from the bottom is allowed (ray model, bottom, Fig. 6, Table I). This identical finding[13,21] is obtained from the Kaneohe source near Oahu (133 Hz, 16 Hz bandwidth, 3709 km section). Is it luck that the subbottom need not be well modeled for these sections, or are other acoustic sections more sensitive to models for propagation in the solid Earth? In any case, the data from the Gulf of Alaska can be used to test the way bottom interactions are modeled near the Kauai source.

ACKNOWLEDGMENTS

This research was supported by the Office of Naval Research (ONR) Contract No. N00014-00-C-0317. John Spiesberger thanks the following individuals and institutions. The data were provided by Jim Phalen of the Applied Physics Laboratory at Johns Hopkins University and Ed McWethy at the ONR. Arthur Bisson at the ONR facilitated access to

these data. Bruce Howe and others at the University of Washington provided information regarding the location and time of the emitted signal. They also deployed the source at Kauai. Bruce Einfalt (Penn State University), Carter Ackerman (Penn State University), and Kurt Metzger (University of Michigan) provided some computer programs used to process the signal for Doppler corrections and replica correlation. This paper is dedicated to Fred Tappert for his scientific contributions and the interesting discussions and collaborations we had over many years, and to Anisim Silivra whom the author worked with on the problem of timing errors in tomography. The author thanks the reviewers for their suggestions.

[1] A. Fabrikant, J. L. Spiesberger, A. Silivra, and H. E. Hurlburt, ''Estimating Climatic Temperature Change in the Ocean with Synthetic Acoustic Apertures,'' IEEE J. Ocean. Eng. **23**(1), 20–25 (1998).

[2] J. L. Spiesberger, H. E. Hurlburt, M. Johnson, M. Keller, S. Meyers, and J. J. O'Brien, ''Acoustic thermometry data compared with two ocean models: The importance of Rossby waves and ENSO in modifying the ocean interior,'' Dyn. Atmos. Oceans **26**, 209–240 (1998).

[3] M. D. Vera, M. A. Dzieciuch, and the NPAL Group, ''Modeling the acoustic receptions at the NPAL array from the Kauai source,'' J. Acoust. Soc. Am. **113**, 2279 (2003).

[4] W. Munk and C. Wunsch, ''Ocean acoustic tomography: A scheme for large scale monitoring,'' Deep-Sea Res., Part A **26**, 123–161 (1979).

[5] B. Cornuelle, W. Munk, and P. Worcester, ''Ocean acoustic tomography from ships,'' J. Geophys. Res. **94**, 6232–6250 (1989).

[6] The AMODE-MST GROUP, ''Moving ship tomography in the North Atlantic,'' EOS Trans. Am. Geophys. Union **75**, 17,21,23 (1994).

[7] T. F. Duda, R. A. Pawlowicz, J. F. Lynch, and B. D. Cornuelle, ''Simulated tomographic reconstruction of ocean features using drifting acoustic receivers and a navigated source,'' J. Acoust. Soc. Am. **98**, 2270–2279 (1995).

[8] J. L. Spiesberger, A. Fabrikant, A. Silivra, and H. E. Hurlburt, ''Mapping Climatic Temperature Changes in the Ocean with Acoustic Tomography: Navigational Requirements,'' IEEE J. Ocean. Eng. **22**(1), 128–142 (1997).

[9] ATOC Instrumentation Group: B. M. Howe, S. G. Anderson, A. B. Baggeroer, J. A. Colosi, K. R. Hardy, D. Horwitt, F. W. Karig, S. Leach, J. A. Mercer, K. Metzger, Jr., L. O. Olson, D. A. Peckham, D. A. Reddaway, R. R. Ryan, R. P. Stein, K. von der Heydt, J. D. Watson, S. L. Weslander, and P. Worcester, ''Instrumentation for the Acoustic Thermometry of Ocean Climate (ATOC) prototype Pacific Ocean network,'' OCEANS 95 Conference Proceedings, San Diego, CA, 9–12 October 1995, pp. 1483–1500.

[10] V. A. Del Grosso, ''New equation for the speed of sound in natural waters with comparisons to other equations,'' J. Acoust. Soc. Am. **56**, 1084–1091 (1974).

[11] S. Levitus, ''Climatological atlas of the world ocean,'' in NOAA Prof. Pap. 13 (U.S. Government Printing Office, Washington, DC, 1982).

[12] C. Garrett and W. Munk, ''Space-time scales of internal waves,'' Geophys. Fluid Dyn. **2**, 225–264 (1972).

[13] M. A. Wolfson and J. L. Spiesberger, ''Full wave simulation of the forward scattering of sound in a structured ocean: A comparison with observations,'' J. Acoust. Soc. Am. **106**, 1293–1306 (1999).

[14] J. A. Colosi, E. K. Scheer, S. M. Flatte, B. D. Cornuelle, M. A. Dzieciuch, W. H. Munk, P. F. Worcester, B. M. Howe, J. A. Mercer, R. C. Spindel, K. Metzger, T. G. Birdsall, and A. B. Baggeroer, ''Comparisons of measured and predicted acoustic fluctuations for a 3250-km propagation experiment in the eastern North Pacific Ocean,'' J. Acoust. Soc. Am. **105**, 3202–3218 (1999).

[15] S. M. Flatte, J. A. Colosi, M. A. Dzieciuch, and P. F. Worcester, ''Acoustic observations of internal-wave strength in the Mid-Pacific in 1989 and 1996,'' J. Acoust. Soc. Am. **100**, 2582 (1996).

[16] J. Simmen, S. M. Flatte, and G. Wang, ''Wavefront folding, chaos, and diffractions for sound propagation through ocean internal waves,'' J. Acoust. Soc. Am. **102**, 239–255 (1997).

[17] V. Renard and J. P. Allenon, ''Sea Beam, multi-beam echo-sounding in 'Jean Charcot': Description, evaluation and first results,'' Int. Hydrogr. Rev. **56**, 35–67 (1979).

[18] National Geophysical Data Center, Boulder, CO, ''5 minute gridded world elevations and bathymetry-a digital database,'' 1987.

[19] F. Tappert, J. L. Spiesberger, and L. Boden, ''New full-wave approximation for ocean acoustic travel time predictions,'' J. Acoust. Soc. Am. **97**, 2771–2782 (1995).

[20] J. B. Bowlin, J. L. Spiesberger, T. F. Duda, and L. E. Freitag, ''Ocean acoustical ray-tracing software RAY,'' Woods Hole Oceanographic Technical Report, WHOI-93-10 (1993).

[21] J. L. Spiesberger and F. D. Tappert, ''Kaneohe acoustic thermometer further validated with rays over 3700 km and the demise of the idea of axially trapped energy,'' J. Acoust. Soc. Am. **99**, 173–184 (1996).

[22] J. L. Spiesberger, ''Ocean acoustic tomography: travel-time biases,'' J. Acoust. Soc. Am. **77**, 83–100 (1985).

[23] A. Draganov and J. Spiesberger, ''Diffraction and pulse delay in a structured ocean,'' J. Acoust. Soc. Am. **98**, 1065–1074 (1995).

[24] A. Silivra, J. L. Spiesberger, A. Fabrikant, and H. E. Hurlburt, ''Acoustic tomography at basin-scales and clock errors,'' IEEE J. Ocean. Eng. **22**(1), 143–150 (1997).

[25] V. H. Lichte, ''Über den Einflußhorizontaler Temperaturschichtung des Seewassers auf die Reichweite von Unterwasserschallsignalen,'' Phys. Z. **17**, 385–389 (1919). English translation by A. F. Wittenborn, with a forward by R. J. Urick is available from Woods Hole Oceanographic Institution, Woods Hole, MA 02543.